 Hot Paper


Alcohol-Induced Conformation Changes and Thermodynamic Signatures in the Binding of Polyphenols to Proline-Rich Salivary Proteins

Nisrine Jahmidi-Azizi,^[a] Rosario Oliva,^{*,[b]} and Roland Winter^{*,[a]}

The first contact of polyphenols (tannins) with the human body occurs in the mouth, where they are known to interact with proline-rich proteins (PRPs). These interactions are important at a sensory level, especially for the development of astringency, but affect also various other biochemical processes. Employing thermodynamic measurements, fluorescence and CD spectroscopy, we investigated the binding process of the prototypical polyphenol ellagic acid (EA) to different IB-PRPs and BSA, also in the presence of ethanol, which is known to influence tannin–protein interactions. Binding of EA to BSA and the small peptide IB7-14 is weak, but very strong to IB9-37. The differences in

binding strength and stoichiometry are due to differences in the binding motifs, which also lead to differences in the thermodynamic signatures of the binding process. EA binding to BSA is enthalpy-driven, whereas binding to both IB7-14 and IB9-37 is entropy-driven. The presence of 10 vol.% EtOH, as present in wines, increases the binding constant of EA with BSA and IB7-14 drastically, but not that with IB9-37; however, it changes the binding stoichiometry. These differences can be attributed to the effect of EtOH on the conformation dynamics of the proteins and to changes in hydration properties in alcoholic solution.

Introduction

Plants contain complex polyphenols, also designated tannins.^[1] They are divided in condensed tannins (or procyanidins), which are polymeric flavan-3-ols, such as catechin and epicatechin produced in grape skins, seeds and stems, and hydrolyzable tannins, such as gallotannins and ellagitannins extracted from oak barrels during wine aging.^[1–4] These compounds may be broadly defined as compounds containing hydroxylated benzene rings with many OH groups allowing them to undergo extensive hydrogen bonding interactions, rendering them also rather water soluble.^[4] Tannins have widely been studied due to their anti-inflammatory, antioxidative and free-radical scavenging properties, and have protective effects against cardiovascular diseases, cancer and other pathological conditions.^[1] They are also used in plants as a defense strategy against pathogens.

Grape seeds contain a large amount of condensed tannins that are largely responsible for the organoleptic properties of

grapes and wines, such as bitterness (e.g., via interaction with taste receptors^[4]), but also for astringency, that is, the dry mouth sensation when drinking very tannic wines. Altogether, there are appreciable levels of tannins in wine, particularly red wine, in the order of 1–6 g L⁻¹.^[1,2,5] Saliva proteins, which lubricate the palate, are thought to be strongly complexed by the polyphenols, even leading to precipitation at high tannin concentrations, resulting in a loss of the lubricating action.^[1–5] During ingestion, tannins interact with many kinds of proteins present in the saliva, stomach, intestines and blood. Next to their interaction with proteins, they are also able to interact with lipid assemblies.^[4]

Human saliva, acting as antimicrobial defense system and lubricant, contains a large body (~40%) of proline-rich proteins (PRPs), which are involved in various enzymatic reactions. Basic PRPs bind polyphenols very efficiently, and the interaction between them and salivary proteins is thought to be the primary source of astringency.^[1] Of note, organoleptic tests showed that astringency is attenuated after eating fatty food or drinking seed oils (the “camembert effect”).^[4]

Beyond the physiological factors that mediate its perception, biophysical quantities (such as binding constants, the driving forces of association, structural changes) are needed to provide solid grounds for a better understanding of the multifaceted properties of PRPs. In the present study, we chose to work on model PRPs of different length, the short peptide IB7-14 and a very long basic peptide, IB9-37, which has 60% of the full length human saliva protein IB9 and serves as a building unit for other members of the family and is hence believed to be a good model protein to follow interactions with polyphenols.^[4–6] IB9-37 is made of three repeated sequences and of PQGPP patterns as depicted in Figure 1. Its structure has been found to be largely random-coil like, with about one third of its residues adopting a type II helix secondary structure.^[6] For

[a] N. Jahmidi-Azizi, Prof. Dr. R. Winter
Physical Chemistry I – Biophysical Chemistry
Department of Chemistry and Chemical Biology
TU Dortmund University
Otto-Hahn Street 4a, 44227 Dortmund (Germany)
E-mail: roland.winter@tu-dortmund.de

[b] Dr. R. Oliva
Department of Chemical Sciences
University of Naples Federico II
Via Cintia 4, 80126 Naples (Italy)
E-mail: rosario.oliva2@unina.it

Supporting information for this article is available on the WWW under <https://doi.org/10.1002/chem.202302384>

© 2023 The Authors. Chemistry - A European Journal published by Wiley-VCH GmbH. This is an open access article under the terms of the Creative Commons Attribution License, which permits use, distribution and reproduction in any medium, provided the original work is properly cited.

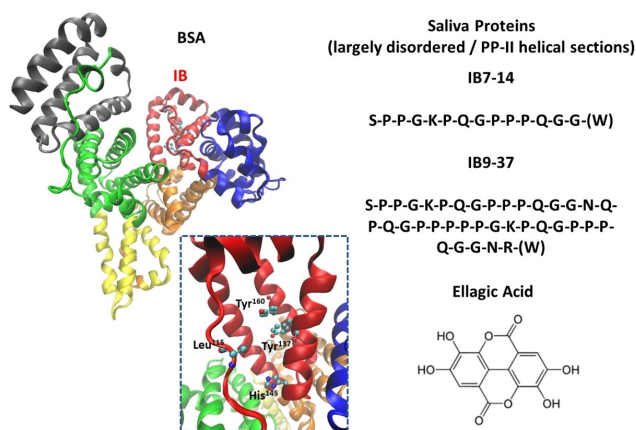


Figure 1. Left: The 3D structure of BSA (PDB ID: 3 V03) represented as ribbon. The different subdomains of the protein are highlighted in different colors: IA (blue), IB (red), IIA (orange), IIB (yellow), IIIA (green), and IIIB (gray).^[9] The four residues that are implicated in the interaction with ellagic acid – Leu115, Try137, His145 and Tyr160, as reported in ref. [13] – are also reported in the structure in balls and stick form. Inset: a magnification of the binding pocket (C atoms in cyan, O atoms in red, and N atoms in blue). The structure was prepared by using VMD software.^[14] Right: the sequences of IB7-14 and IB9-37. The two proteins mainly adopt a disordered structure in solution. The Trp residues are reported in brackets since they are not part of the sequence of saliva proteins, they were added for concentration determination, only. Bottom right: the chemical structure of ellagic acid. EA has four hydroxy residues and two acyloxy groups connected to a core of fused aromatic rings.

comparison with a properly folded abundant protein, we used the standard test-case protein bovine serum albumin (BSA).^[7,8] Albumins are the most common proteins in the blood stream, and they bind and transport various exogenous and endogenous molecules, including tannins. Oenologists use egg albumins to filter excess tannins in wine by sedimentation (“fining”). BSA has a similar structure as human serum albumin (HSA) and is made up of three homologous domains which are divided into nine loops, and has two Trp residues. Quenching of Trp fluorescence has been observed mainly upon binding of tannins to BSA and HSA.⁷

As prototypical polyphenolic binding partner we used ellagic acid (EA), a polyphenol found in many fruits, including grapes, seeds, and vegetables,^[1] but also in oak species (about 80 mg L⁻¹ in oak-aged red wine). Ellagic acid is the dilactone of hexahydroxydiphenic acid (Figure 1), and plants produce it from hydrolysis of tannins such as ellagitannin.

Fluorescence spectroscopy experiments were carried out to evaluate the binding constant of complex formation and its stoichiometry. Measuring the heat transfer during the interaction between the polyphenol and the proteins allowed us to determine the enthalpy and entropy changes upon binding, providing important information about the binding mechanism.^[9] By measuring the pressure dependence of the binding process, additional mechanistic information could be extracted from the volumetric data obtained. Complementary circular dichroism (CD) spectroscopy informed about structural changes upon binding (see the Supporting Information for experimental details). This multi-technique approach enabled us to obtain a comprehensive description of the binding

process, revealing the underpinning molecular determinants governing the complex formation. As the solvent composition, in particular the presence of alcohol, can influence the polyphenol-protein interaction and astringency,^[10] we studied also the effect of 10 vol.% ethanol, a typical concentration in wines (corresponding to ~80 g L⁻¹), on the binding process.

Results

The strength of the interaction between the ellagic acid (EA) and the proteins (BSA, IB7-14 and IB9-37, see Figure 1 for the 3D structure of BSA, the sequences of the intrinsically disordered peptides IB7-14 and IB9-37, and the chemical structure of EA) and the impact of alcoholic solution, containing 10 vol.% ethanol, on the complex formation was explored by means of steady-state fluorescence spectroscopy. To this end, a solution at fixed concentration of EA was titrated with a solution of the proteins. The ligand EA is basically not fluorescent in solution.^[13] We found that, upon interaction with the proteins, an increase of fluorescence intensity occurred (see Figure S1 in the Supporting Information, where spectra of EA at different BSA concentrations are reported as an example), a behavior very similar to that to the well-known fluorophore 8-anilinonaphthalene-1-sulfonic acid (ANS).^[15] Thus, in the present case, fluorescence spectroscopy is very suitable for detecting the binding between EA and the proteins, since the intensity is directly related to the degree of binding. Figure 2 shows the binding isotherms in neat buffer and in the presence of 10 vol.% EtOH, at ambient conditions of $T=25^{\circ}\text{C}$ and $p=1$ bar. The binding constants obtained after fitting the data are reported in Table 1.

In order to evaluate the strength of the complex formed, described by the binding constant K_b , the experimental data were fitted with a suitable binding model.^[16,17] In the present case, the data at neat buffer conditions could be well fitted using a 1:1 binding model for the interaction of EA with BSA, that is, it is assumed that one molecule of EA interacts with one molecule of protein. An 1:1 stoichiometry for the complex formation between EA and BSA was also previously reported.^[13] For polyproline saliva proteins, the binding motif has been proposed to be the PQGPP sequence.^[6] As the IB7-14 possesses only one such motif, it is reasonable to assume that also in this case 1:1 binding takes place. Conversely, for IB9-37 in neat buffer solution, we found best fits assuming that two molecules of EA bind to one molecule of protein. An inspection of the data reported in Table 1 reveals that, under neat buffer conditions, the interaction between EA and proteins is quite weak, with a K_b value of the order of 10^3 M⁻¹ for BSA and IB7-14. Conversely, for IB9-37, rather strong binding occurred (~ 10^6 M⁻¹). Thus, from the data reported in Table 1 it is clear that EA has the strongest affinity for IB9-37, followed by IB7-14 and finally BSA.

Next, we explored the impact of the presence of ethanol on the complex formation. To this end, the binding experiments were performed in the presence of 10 vol% EtOH, a typical concentration found in wines. The binding isotherms obtained

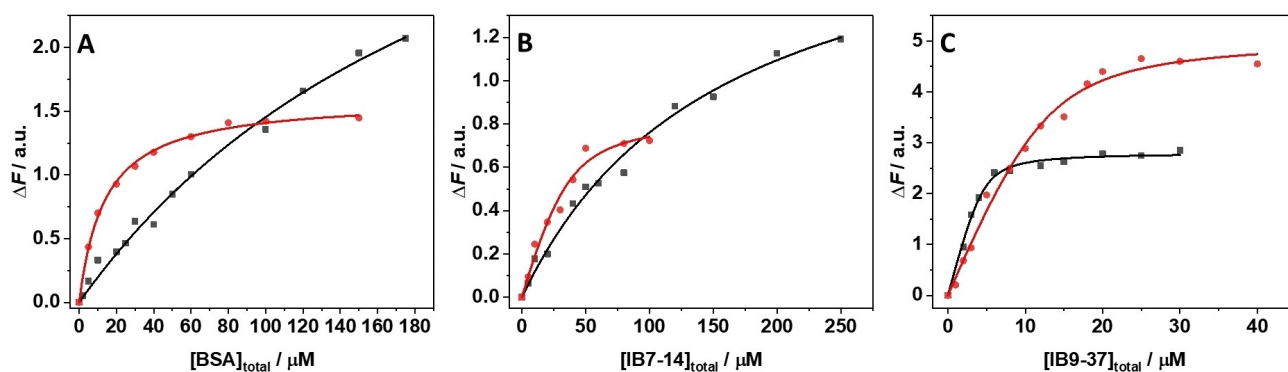


Figure 2. Binding isotherms obtained by means of steady-state fluorescence spectroscopy for complex formation between ellagic acid and A) BSA, B) IB7-14, and C) IB9-37 in neat buffer (●) and in the presence of 10 vol.% EtOH (■). All the experiments were performed at 25 °C, in 20 mM Tris-HCl buffer (pH 7.4). The solid lines are the best fit of experimental data according to a 1:1 binding model (1:2 for the IB9-37:EA system at neat buffer conditions).

Tris-HCl, pH 7.4			Tris-HCl, ethanol 10% vol., pH 7.4		
System	p [bar]	K_b [M^{-1}]	System	p [bar]	K_b [M^{-1}]
BSA/EA	1	$(5.5 \pm 0.9) \cdot 10^3$	BSA/EA	1	$(1.4 \pm 0.3) \cdot 10^5$
	500	$(3.5 \pm 0.2) \cdot 10^3$		500	$(1.3 \pm 0.2) \cdot 10^5$
	1000	$(3.4 \pm 1.0) \cdot 10^3$		1000	$(1.3 \pm 0.2) \cdot 10^5$
	1500	$(0.82 \pm 0.55) \cdot 10^3$		1500	$(0.76 \pm 0.41) \cdot 10^5$
	2000	$(0.81 \pm 0.33) \cdot 10^3$		2000	$(0.71 \pm 0.22) \cdot 10^5$
ΔV_b° [$mL\ mol^{-1}$]	28.3 ± 8.1		ΔV_b° [$mL\ mol^{-1}$]	9.9 ± 2.2	
IB7-14/EA	1	$(6.0 \pm 1.1) \cdot 10^3$	IB7-14/EA	1	$(4.3 \pm 1.3) \cdot 10^4$
	500	$(6.2 \pm 2.5) \cdot 10^3$		500	$(4.3 \pm 1.0) \cdot 10^4$
	1000	$(6.8 \pm 1.5) \cdot 10^3$		1000	$(2.4 \pm 0.6) \cdot 10^4$
	1500	$(6.8 \pm 1.4) \cdot 10^3$		1500	$(2.4 \pm 0.8) \cdot 10^4$
	2000	$(6.1 \pm 1.2) \cdot 10^3$		2000	$(2.3 \pm 0.5) \cdot 10^4$
ΔV_b° [$mL\ mol^{-1}$]	≈ 0		ΔV_b° [$mL\ mol^{-1}$]	9.1 ± 2.6	
IB9-37/EA ^[a]	1	$(1.2 \pm 0.9) \cdot 10^6$	IB9-37/EA	1	$(0.86 \pm 0.35) \cdot 10^6$
	500	$(3.3 \pm 1.5) \cdot 10^6$		500	$(2.5 \pm 1.4) \cdot 10^6$
	1000	$(1.0 \pm 0.4) \cdot 10^6$		1000	$(2.1 \pm 1.0) \cdot 10^6$
	1500	$(3.1 \pm 2.0) \cdot 10^6$		1500	$(2.4 \pm 0.8) \cdot 10^6$
	2000	$(1.1 \pm 0.4) \cdot 10^6$		2000	$(2.7 \pm 1.2) \cdot 10^6$
ΔV_b° [$mL\ mol^{-1}$]	≈ 0		ΔV_b° [$mL\ mol^{-1}$]	-10.2 ± 6.1	

[a] For this system, the IB9-37/EA stoichiometry was 1:2.

are depicted in Figure 1 (red lines). The values of the binding constants are reported on the right side of Table 1. The data reveal that the presence of ethanol has a strong impact on the complex formation between BSA and EA. Interestingly, a marked increase of K_b (ca. 26 times) was determined, indicating that ethanol strongly enhances the binding of EA to BSA. The same effect was also observed for IB7-14. However, the observed increase of K_b was lower, around seven times. Conversely, it seems that ethanol has no significant effects on the binding between EA and IB9-37. The K_b value obtained is very similar (within the experimental error) to that obtained in the absence of ethanol.

To shed more light in the observed differences in the affinities of EA for the three proteins and the dependence of K_b on ethanol, we performed isothermal titration calorimetry (ITC) measurements. In this way, the thermodynamic signature of the complex formation could be explored. Indeed, the determination of thermodynamic parameters of interaction were useful in rationalizing our findings. Figure 3 and Table S1 summarize the thermodynamic parameters for the complex formation between EA and the employed proteins. The ITC traces obtained when the proteins were titrated into a solution of EA in neat buffer and in the presence of ethanol are reported in Figures S2 and S3, respectively.

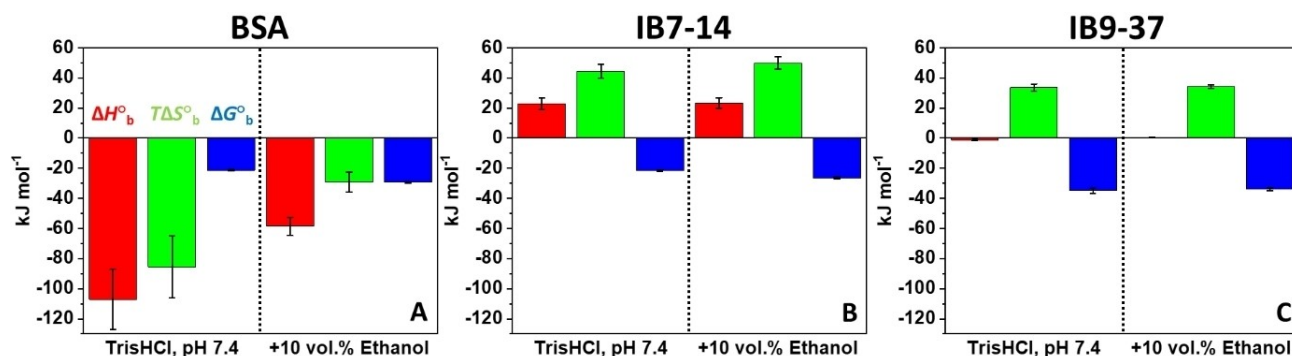


Figure 3. Thermodynamic parameters, at 25 °C and 1 bar, for the complex formation between EA and A) BSA, B) IB7-14, and C) IB9-37 in 20 mM Tris-HCl buffer (pH 7.4), and in the presence of 10 vol.% EtOH. The standard enthalpy change of binding, ΔH°_b , is reported in red, the binding entropy, $T\Delta S^{\circ}_b$, in green, and the binding Gibbs energy, ΔG°_b , is reported in blue. Note that the ΔH°_b for the EA/IB9-37 complex formation is close to zero. ΔH°_b was obtained from ITC experiments reported in Figures S2 and S3. ΔG°_b was obtained from the values of the binding constants reported in Table 1, using the relation $\Delta G^{\circ}_b = -RT\ln(K_b)$. The $T\Delta S^{\circ}_b$ value was determined from the Gibbs-Helmholtz equation $\Delta G^{\circ}_b = \Delta H^{\circ}_b - T\Delta S^{\circ}_b$.

As the K_b values are quite small for the EA/BSA and EA/IB7-14 complex formation, ITC cannot be performed in the usual way to determine the binding constants.^[18] However, the enthalpy change upon complex formation could be determined in the following way. The calorimetry vessel was filled with an excess of the ligand EA, and the proteins were placed in the syringe. Then, small amounts of protein (20 μ L) were injected into the vessel. At these conditions, a sequence of similar peaks should be obtained. The recorded heats, normalized by the moles of bound protein, which can be calculated from the binding constants (Table 1), gave the enthalpy change for the complex formation, ΔH°_b . The same procedure was used for the protein IB9-37.

The data reported in Figure 3 and Table S2 reveal that for the complex formation between EA and BSA, the enthalpy change is negative, suggesting formation of favorable non-covalent intermolecular interactions bonds (e.g., hydrogen bonds) between the ligand and the protein. The entropy change is negative as well, suggesting a reduction of the degree of freedom of the system, contributing in an unfavorable way to ΔG°_b . The negative ΔS°_b can be ascribed to the reduction of fluctuations of the protein structure upon binding. Surprisingly, in the presence of ethanol, the ΔH°_b value

increased, indicating weaker intermolecular interactions upon binding with respect to neat buffer. However, the binding entropy changed significantly, moving towards a more positive and hence favorable value, which explains the marked increase of K_b in alcoholic solution.

For IB7-14 in neat buffer, both the enthalpy and entropy changes are positive, thus indicating that the binding process is entropically driven. These data suggest that upon binding the breakup and release of hydration water surrounding the interacting partners occurred. Similar results were obtained in the presence of ethanol. The entropy change was slightly more positive, however, which contributes to the observed increase of the binding constant. For IB9-37, the thermodynamic signature of complex formation with EA is completely different. In neat buffer, the enthalpy change was found to be very small, close to zero, meaning that the binding is totally driven by an increase in entropy. In the presence of EtOH, similar results were obtained, which agree with the small effect of ethanol on the complex formation observed in the titration experiments.

Next, in order to reveal possible conformational changes of the proteins imposed by the presence of EtOH and upon EA binding, circular dichroism (CD) spectroscopic experiments were carried out.^[19–21] Figure 4 shows the CD spectra of BSA,

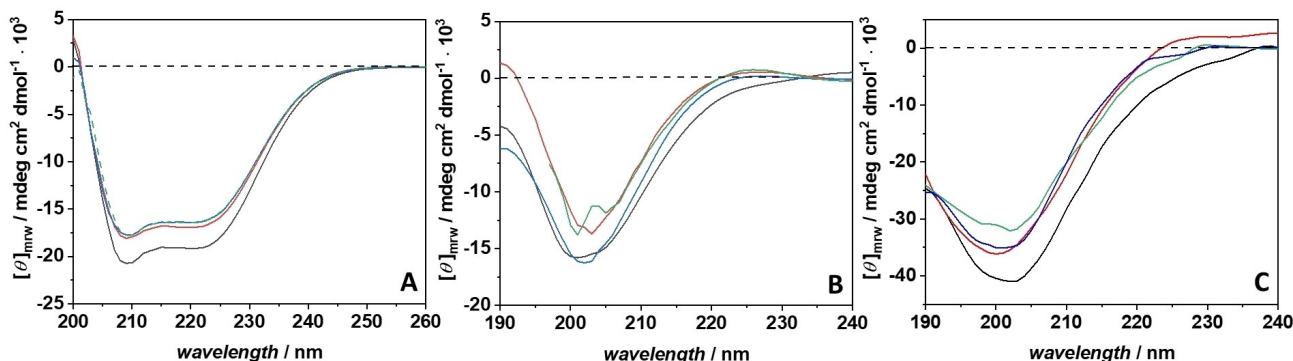


Figure 4. CD spectra of A) BSA, B) IB7-14, and C) IB9-37 at the following conditions: neat buffer (—), with EA in neat buffer (—), in the presence of 10 vol.% EtOH (—), and with EA in the presence of 10 vol.% EtOH (—). Please note that for BSA, the green and blue lines are almost superimposed. All the experiments were performed in 20 mM Tris-HCl buffer (pH 7.4) at 25 °C and 1 bar.

IB7-14, and IB9-37 in the absence and presence of the ligand EA under both neat buffer conditions and upon addition of 10 vol.% EtOH.

The CD spectrum of BSA in neat buffer (Figure 4A) is characterized by two minima, located at ~ 222 and ~ 209 nm, and a positive band raising at 200 nm. These features are indicative of a protein adopting mainly an α -helical structure, in agreement with previously reported data and the crystal structure of BSA.^[12,18] Upon addition of EA, the general shape of the spectrum was unaffected. However, the intensity of the two negative bands decreased. This could be due to a small conformational change in the secondary structure content, such as a small decrease of α -helical conformations imposed by binding of the ligand. In the presence of 10 vol.% EtOH, a reduction of the spectral intensity was observed with respect to the neat buffer conditions, indicating that also ethanol, at this concentration, is able to slightly change the secondary structure of the protein, possibly increasing the fraction of disordered conformations, as previously reported.^[22] Upon addition of EA in the presence of EtOH, no change in the shape or intensity of the CD spectrum was detected.

The small peptide IB7-14 showed a CD spectrum in neat buffer with a minimum around 203 nm, in agreement with previously reported data.^[23] Below 200 nm, the intensity increased, moving towards positive values, and another weak band emerged around 220 nm. These features are indicative of the presence of a polyproline II (PP-II) helix. The minimum around 200 nm is indicative of a random-coil structure.^[6,24] We can thus infer that IB7-14 is not completely folded in a PP-II helical type of structure, but still largely disordered, as previously reported.^[6] Upon addition of EA, the intensity of the minimum decreased and shifted slightly to larger wavelengths, the intensity at 220 nm becoming more pronounced and that below 200 nm increased. Thus, it seems that IB7-14 is adopting a slightly more ordered structure, most likely by an increase of the PP-II conformation. In the presence of EtOH, the recorded spectrum was qualitatively similar to that at neat buffer conditions, the intensity at 220 nm was more evident only, indicating that the population of PP-II is higher. Upon addition

of EA, the spectrum was very similar to that recorded in buffer with EA. Thus, we can conclude that EA in both solvents caused a small conformational change of IB7-14, promoting most likely a more ordered PP-II conformation. The observed changes are very small, however.

The spectrum of the longer polypeptide IB9-37 in neat buffer (black spectrum) showed the features of a random-coil structure, with a minimum around 200 nm, in agreement with previous data.^[4] Upon binding of EA, only small changes were observed. In the presence of 10 vol.% EtOH, the spectrum of IB9-37 with and without EA are superimposable, indicating that no significant conformational changes occurred. We can therefore conclude that IB9-37 largely retains its random-coil conformation upon binding of EA under both solvent conditions.

Finally, to gain further insights into the molecular determinants underlying the complex formation, binding experiments were also performed under high pressure, up to 2000 bar, by means of high hydrostatic pressure (HHP) fluorescence methodology. Figure 5 shows the binding isotherms obtained for the complex formation between BSA and EA in the pressure range 1–2000 bar, in neat buffer and in the presence of 10 vol.% EtOH. The pressure dependent binding curves for the other systems are reported in Figure S3. Table 1 shows the K_b values as a function of pressure.

Inspection of Table 1 reveals that for the EA-BSA complex formation, a marked decrease of the K_b value upon pressurization (of about 6.8 times at 2000 bar with respect to K_b at 1 bar) is observed, that is, pressure does not favor the complex formation. In the presence of EtOH, again a decrease of K_b with pressure was observed. However, the decrease in ethanolic solution was less pronounced, about two times at 2000 bar with respect the value at 1 bar. A completely different scenario was observed for the complex formation between EA and the saliva protein IB7-14. Upon increasing pressure from 1 bar to 2000 bar, no significant changes of K_b were observed, which remained essentially constant over the whole pressure range covered. Interestingly, in the presence of EtOH, the system became pressure-sensitive and a significant decrease of the

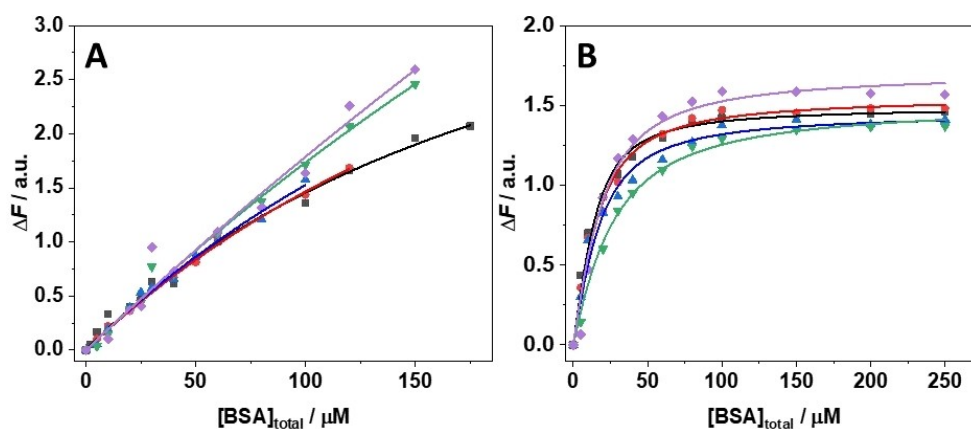


Figure 5. Binding isotherms obtained by means of HHP steady-state fluorescence spectroscopy for the complex formation between ellagic acid and BSA in A) neat buffer and B) in the presence of 10 vol.% EtOH at 1 bar (○), 500 bar (●), 1000 bar (▲), 1500 bar (○), and 2000 bar (●). All the experiments were performed at 25 °C in 20 mM Tris-HCl buffer (pH 7.4). The solid lines are the best fits of the experimental data according to a 1:1 binding model.

binding constant with pressure was again observed. For IB9-37 in pure buffer solution, K_b remained roughly constant in the whole pressure range explored, but increased slightly in the presence of EtOH.

From the pressure dependence of K_b , it was possible to calculate the volume change accompanying the complexation reaction,^[25,26] according to $(\ln K_b/dp)_T = -\Delta V_b^\circ/(RT)$, where ΔV_b° is the binding volume, which is defined as the difference between the partial molar volume of the ligand-protein complex and the sum of the partial molar volumes of the ligand and of the protein. According to the Le Châtelier principle, pressure favors the state that occupies the smallest possible overall volume.^[15,25,26] Thus, if pressure favors the formation of the complex, ΔV_b° will be negative, and vice versa. Figure 6 shows the plots of $\ln(K_b)$ versus p , from which the ΔV_b° values were determined (Table 1).

The data reported in Table 1 show that the binding volume is positive for the serum protein BSA under both solution conditions, highlighting quantitatively that the pressure is not favoring the complex formation ($V_{\text{complex}} > V_{\text{ligand}} + V_{\text{protein}}$). It is remarkable that the binding volume in the presence EtOH is three times lower compared to that obtained in neat buffer. Conversely, for the IB7-14 protein in neat buffer conditions, ΔV_b° is essentially zero, in other words, the complex formation is pressure insensitive. In the presence of EtOH, ΔV_b° becomes positive. For IB9-37, it was found that the binding volume is close to zero (within the experimental error) in neat buffer, as in the case of the shorter peptide IB7-14. Conversely, in alcoholic solution, in sharp contrast to the result obtained for IB7-14, ΔV_b° becomes negative, revealing that the complex occupies a smaller partial molar volume with respect to the uncomplexed state, thus favoring formation of the complex.

Discussion

The results obtained show that the binding of the polyphenol EA to the three proteins employed is characterized by different binding constants (strength). At ambient conditions and in neat buffer, the binding constant K_b follows the order IB9-37 \gg IB7-

14 \approx BSA. This is a remarkable result for several reasons. First of all, BSA is a compact folded protein which is adopting a well-defined three-dimensional structure, providing binding pockets able to accommodate the ligand. Instead, the two saliva proteins are mainly unstructured and lack defined binding pockets. Despite of this fact, the binding constants of EA for BSA is similar to that for IB7-14 ($\sim 10^3 \text{ M}^{-1}$), but is remarkably higher for IB9-37 ($\sim 10^6 \text{ M}^{-1}$). Secondly, the K_b value of EA for IB9-37 is ~ 200 times higher than that obtained for the smaller peptide IB7-14. A higher affinity for longer saliva proteins was also reported for other tannins.^[4,5] Further, we found that two EA molecules can bind to IB9-37. Instead, for IB7-14, the binding stoichiometry is 1:1. These results indicate that significant differences in the chemical makeup of the binding site(s) involved should be present.

The binding site of EA to BSA was previously identified by molecular docking studies.^[13] It was found that EA is bound in the subdomain IB of BSA to the residues Tyr160, Tyr137, Leu115, and His145 (Figure 1). The binding is accompanied by small conformational changes. Conversely, for the saliva proteins, the ability to bind tannins is generally attributed to the presence of the PQGPP motif.^[6] In this case, a polyphenol, like EA, can establish hydrophobic interactions with the ring of the proline residues and hydrogen bonds with the carbonyl group of prolines and peptide bonds.^[23,28] In the sequence of IB7-14 and IB9-37, one and two such motifs are present, respectively, which would be in line with our binding data, revealing stoichiometries of 1:1 and 1:2 (protein/EA) for the short and long polypeptide, respectively. However, the binding constants obtained were completely different (Table 1). If binding would occur by the PQGPP motif only, a similar value of K_b should be obtained for the two polypeptides (in particular as the two polypeptides are essentially disordered and the structure does not change significantly upon binding of EA), which is not the case. The primary sequence of IB9-37 contains a motif composed of five Pro residues (PPPPP) in addition to the PQGPP motif, which could be implicated in the binding. In the sequence of IB7-14, such motif is missing. Hence, we may assume that in the case of IB7-14, the binding of EA occurs effectively to the PQGPP motif only, with a K_b of about 10^3 M^{-1} ,

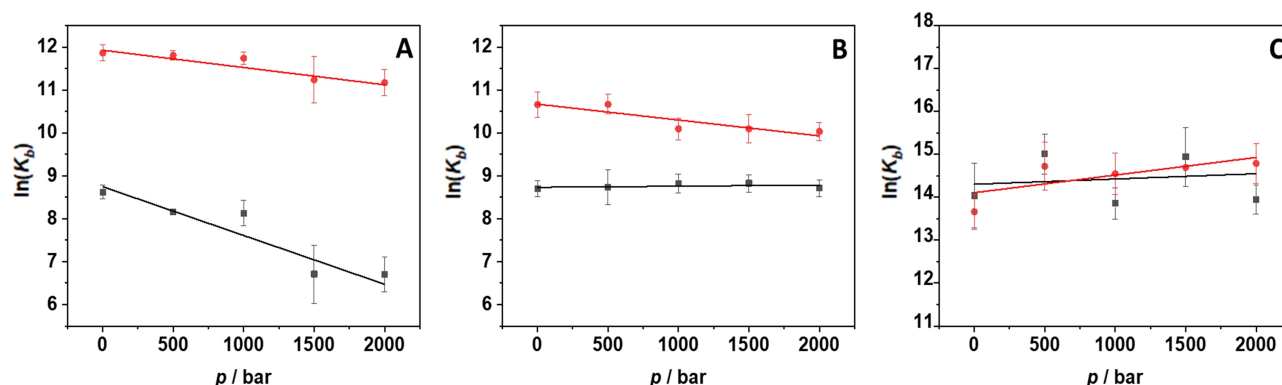


Figure 6. Plots of $\ln(K_b)$ vs. p for complex formation between EA and A) BSA, B) IB7-14, and C) IB9-37 in neat buffer (□) and in the presence of 10 vol.% EtOH (●). All experiments were performed at 25 °C, in 20 mM Tris-HCl buffer (pH 7.4). The value of the standard binding volume, ΔV_b° , was determined from the slopes of the plots ($-\Delta V_b^\circ/RT$).

and for IB9-37, binding to both PQGPP and PPTPP motifs could take place. In this case, the data should be fitted with a model predicting the presence of two sites characterized by two different binding constants,^[15–17] which is in disagreement with our data, however. Consequentially, the most probable scenario is that two EA molecules bind strongly (employing stacking of the phenol groups on EA against the pyrrolidone ring of proline through σ - π attraction, and formation of H-bonds between phenolic hydroxy groups and carbonyl groups linked to proline amino groups) to the same PPTPP motif in IB9-37, which is characterized by a high affinity. This explanation is also supported by the observation that the thermodynamic data obtained by ITC (Figure 3 and Table S1) show that the energetics of complex formation is different for the two peptides. The binding enthalpy, ΔH_{br}° , is $\sim 22 \text{ kJ mol}^{-1}$ for IB7-14, and close to zero for IB9-37. This is clear evidence that the residues involved in the complex formation of the two proteins are not the same.

Of note, it has been reported that the higher affinity of tannins for longer saliva proteins (compared to short ones) can be attributed to the “wrapping” of the longer protein around the ligand.^[4,5] In this case, the protein changes its conformation, adopting a more compact structure. However, our CD data show that such conformational changes do not seem to occur in the IB9-37 structure upon binding of EA. Moreover, the conformational change should contribute negatively to the binding entropy, which contrasts with our findings.

The comparison of the thermodynamic binding data reported in Figure 3 reveals important information on the role of hydration in driving the complex formation under neat buffer conditions.^[26,29] In the case of BSA, the enthalpy change upon binding is negative, the entropy change is negative as well, thus the binding is enthalpically driven. For IB7-14, ΔH_{br}° is positive, but $\Delta H_{br}^{\circ} = -1 \text{ kJ mol}^{-1}$, that is, is essentially zero for IB9-37. This is to say, the binding process is entropically driven in both cases. The saliva proteins, lacking folded structures, expose their residues to the aqueous solvent. Thus, upon binding, the release of hydration water and the consequentially increase of entropy is expected to dominate the binding. Instead, for BSA, just few molecules of water are present in the hydrophobic pocket, rendering significant dehydration upon binding less likely. This highlights the importance of the entropic contribution in driving complex formation even in the absence of a defined binding pocket.

The high-pressure binding data revealed that the binding volume (Table 1) for the interaction of EA with BSA is positive, indicating that the complex occupies a larger volume with respect to the uncomplexed state. A $\Delta V_b^{\circ} > 0$ can be ascribed to an increase of void volume in the binding pocket upon complex formation and/or the release of hydration water to the bulk solvent.^[15,18,25] Instead, for IB7-14, the binding volume is essentially zero, revealing an almost perfect packing between the interacting partners. The same behavior was observed for the longer IB9-37. A $\Delta V_b^{\circ} \approx 0 \text{ mL mol}^{-1}$ value could be due to the presence of two opposite contributing factors: the release of hydration water to the bulk (contributing positively to the ΔV_b° as hydration water has a slightly larger density due to the

electrostrictive effect^[27]) and the reduction of the fluctuations of the protein structure upon binding (contributing negatively to ΔV_b°).^[27] In our case, for IB7-14 and IB9-37, these two contributions seem to cancel each other largely, resulting in an almost pressure-insensitive binding constant.

The presence of 10 vol.% EtOH in the aqueous solution affects the binding constant of EA for the BSA and IB7-14 significantly, but not that for IB9-37. In the presence of ethanol, the K_b value of EA for BSA increased from $5.5 \times 10^3 \text{ M}^{-1}$ to $1.4 \times 10^5 \text{ M}^{-1}$, that is, EtOH promotes the complex formation drastically. It is known that ethanol can cause protein denaturation at high concentrations.^[22,30] Thus, it is possible that in 10 vol.% alcoholic solution, BSA adopts a slightly more open structure, favoring the entrance of EA into the binding pocket by increased conformational fluctuations. Indeed, the CD data revealed a small, but significant conformational change of the protein structure. A contribution to the increase of K_b could also come from the more positive entropy change inferred from the ITC experiments. In neat buffer, $T\Delta S_b^{\circ}$ is -85 kJ mol^{-1} , but increases to -29 kJ mol^{-1} in 10 vol.% EtOH. Thus, the entropy penalty to be paid by the complex formation is strongly reduced. This could be ascribed to an increase in conformational fluctuations induced by the presence of EtOH which is preserved upon binding. A positive contribution to the entropy change could also come from the release of hydration water upon complex formation. Indeed, through MD simulation it was found that the number of hydrogen bonds formed between chymotrypsin inhibitor 2 and water molecules is larger in water/ethanol mixture (10 vol.%) with respect to bulk water.^[31] Thus, in the presence of ethanol, more water molecules may be released upon complex formation, rendering the entropic contribution more favorable in comparison to neat buffer. Such scenario should lead to a larger binding volume with respect to that observed in neat buffer, as in fact observed. Of note, it was found that ethanol may bind directly to BSA, decreasing the affinity of small ligands, such as ANS, to the protein.^[32] The reduction of affinity was attributed to the binding of the alcohol in the hydrophobic pockets where also ANS is localized, acting as competitor. However, in the present case, an increase of the binding constant was observed, indicating that ethanol is not bound to the site where EA is located.

Very curiously, it was found that ethanol strongly enhances the affinity of EA for IB7-14, but not for IB9-37 (Table 1). This is another, indirect, proof that the residues involved in the interaction of EA with the two saliva proteins are not the same. Because very small conformational changes were found in case of IB7-14 upon EA binding and in the presence of ethanol (Figure 4), the observed increase of K_b for the complex formation between IB7-14 and EA could be due to the role played by the hydration water. As discussed above, it was found that the number of hydrogen bonds between proteins and water molecules is higher in 10 vol.% EtOH solution with respect to neat water alone.^[31] Hence, the major contribution to binding could come from the release of hydration water from the binding site upon EA interaction, leading to an increase in entropy, in agreement with the increased entropy change upon binding found in the presence of ethanol (Figure 3 and

Table S1). This would be in line with the HHP experiments, which showed that in going from buffer to alcoholic solution, the binding volume, ΔV_b° , increased from ~ 0 to 9.1 mL mol^{-1} , which is likely due to the release of more hydration water to the bulk.

Conversely, for IB9-37, ethanol had basically no effect on the value of the binding constant. Also, the binding volume is very similar to that obtained under neat buffer conditions. In this case, it is most likely that the local hydration at the level of the involved residues is not the same in the two polypeptides. Thus, their response to changes in the solvent conditions (addition of 10 vol.% EtOH) is expected to be unlike, explaining the observed differences. Remarkably, for IB9-37, a change in the stoichiometry was found by changing the solvent from neat buffer to 10 vol.% EtOH solution. Two EA molecules were found to bind to IB9-37 in buffer, but only one in the presence of EtOH. It has been reported that ethanol has a preference to bind to Val and Pro residues in random-coil structures.^[33] Thus, most likely, the decrease of stoichiometry is due to direct binding of ethanol to some of the Pro residues involved in the binding, hampering the interaction of a second EA molecule.

For completeness, it should be mentioned that another factor could contribute to the observed thermodynamic parameters. In discussing the enthalpy, entropy and volume changes upon binding with and without ethanol, the above discussion focused on interactions of the ligand with the protein sites and water being released from them. In addition, changes in partial molar enthalpy, entropy, and volume (due to changes of the hydration volume) of the ligand could play a role upon addition of 10 vol.% EtOH to the solution. In other words, the activity (coefficient) of the ligand would change with the addition of EtOH. However, this effect could be small.

Conclusions

Our results show that binding of the polyphenol ellagic acid (EA) to the three proteins employed is characterized by different binding constants (strengths) and binding stoichiometries. The binding of EA to BSA and the small saliva peptide IB7-14 is weak, but very strong to IB9-37. The differences in binding strength and stoichiometry are due to differences in the chemical make-up of the binding motifs of the proteins; these also lead to marked differences in the thermodynamic signatures of the binding process. Binding of EA to BSA is enthalpy-driven and the binding volume is positive. In contrast, binding of EA to both IB7-14 and IB9-37 is essentially entropy-driven, most likely due to the dislodgement of structured hydration water molecules on the protein and on the polyphenol as a result of some hydrophobic effect toward protein nonpolar residues. For the saliva proteins, the binding volume is essentially zero, revealing an almost perfect packing between the interacting partners. Ethanol can alter both protein structure and polyphenol–protein interactions, for example, through disruption of hydrogen bonding. The presence of 10 vol.% EtOH increases the binding constant of EA to BSA and IB7-14 drastically, essentially due to an increase of the binding

entropy, but not that to IB9-37, whose binding stoichiometry, however, changes in alcoholic solution. The differences can be attributed to the effect of EtOH on the conformational fluctuations of BSA, to binding of EtOH to Pro residues, and to differences in hydration properties of the saliva peptides in alcoholic solution, as also suggested by the changes in their binding volumes.

Due to the large variety of salivary proteins and enormous complexity of polyphenolic compounds in grapes and wines, it is a formidable task to comprehend their organoleptic properties and biochemical processes at the molecular level. Here, we have shown how drastically the presence of ethanol at wine-relevant concentrations can affect the underlying mechanism of interaction of a prototypical polyphenol with salivary proteins. Dietary oils in fatty food are thought to alter such interactions, leading to a decrease of perception of astringency via preferential polyphenol–lipid interactions.^[4]

Experimental Section

Reagents: The proteins bovine serum albumin (BSA, molecular weight of 66 463 Da, 583 residues) in the form of lyophilized powder, the tannin ellagic acid (EA) and ethanol were all purchased from Sigma–Aldrich. Saliva peptides IB7-14 (primary sequence: SPPGKPPQGGW, molecular weight of 1486.63 Da) and IB9-37 (primary sequence: SPPGKPPQGGNQPQGGPPPPGKPPQGGNRW, molecular weight of 3768.12 Da) were purchased from GenScript (Leiden, Netherlands). All the sample solutions were prepared in the pressure-stable 20 mM Tris-HCl buffer (pH 7.4). Deionized water was used for all buffer and sample preparations.

Samples preparation: The Tris-HCl buffer used for all experiments was adjusted to a pH of 7.4 by addition of HCl and filtered with a syringe filter with a cutoff of $0.45 \mu\text{m}$. The stock solution of the proteins BSA, and IB7-14 and IB9-37 were prepared by dissolving the lyophilized powder in Tris-HCl buffer. By measuring the absorbance at 280 nm with a UV-1800 spectrometer from Shimadzu Corporation (Kyoto, Japan), and using a molar extinction coefficient of $43600 \text{ M}^{-1} \text{ cm}^{-1}$ for BSA, and $5600 \text{ M}^{-1} \text{ cm}^{-1}$ for IB7-14 and IB9-37, the exact concentrations of the proteins were determined.^[15,18] The saliva proteins do not have any Trp residue in their primary sequence. Hence, a Trp residue was added in order to evaluate exactly their concentrations from UV/Vis spectrophotometry. A concentrated stock solution of ellagic acid was prepared by weighing and dissolving it in 0.1 M NaOH solution. The usual concentration of the prepared stock solutions was 10 mM.

Steady-state fluorescence spectroscopy: The extent of complex formation between EA and BSA, IB7-14, and IB9-37 was followed by means of steady-state fluorescence spectroscopy using a K2 fluorometer from ISS, Inc. (Champaign, IL, USA). The binding isotherms were obtained by recording EA emission spectra by exciting the solutions at 371 nm and recording the emission intensities in the range 400–550 nm. At this wavelength, no interference from the proteins is present. The slit widths of the excitation and emission monochromators were both set to 8 nm. Briefly, a series of solutions with a fixed concentration of EA at $15 \mu\text{M}$ were prepared, and the concentration of proteins was varied between 0 and ~ 180 , ~ 250 , and $\sim 40 \mu\text{M}$ for the titration with BSA, IB7-14, and IB9-37, respectively. Determination of the binding constants, K_b , was performed by using a plot of $\Delta F = F - F_0$ (where F is the fluorescence intensity of EA at its maximum in the presence of protein, and F_0 is the intensity of EA in the absence of protein) as

a function of total protein concentration, as previously described in.^[15] The data were analyzed assuming a 1:1 stoichiometry for all the systems except for the titration with IB9-37 in neat buffer, where the stoichiometry was found to be 1:2 (IB9-37:EA). For the pressure dependent measurements, the high-pressure cell from ISS and quartz cuvettes were used. The pressure was controlled by means of a manual pump, and water was used as pressurizing fluid. A pressure range from 1 to 2000 bar was explored. The EA and protein solutions were mixed, vortexed, and then filled into the sample cell, which was sealed with DuraSeal™ laboratory stretch film and placed into the high-pressure vessel. The stretch film allowed fast pressure transmission in the sample cuvette. The reported values of the binding constants obtained from the fluorescence experiments are the average of at least three independent experiments performed with freshly prepared samples.

Circular dichroism spectroscopy: CD spectroscopy experiments were performed in the Far-UV region (190–260 nm) in order to determine the secondary structure of the proteins and the impact on it of 10 vol.% ethanol and EA. The CD spectra of 15 μM BSA and IB7-14 and 20 μM IB9-37 in the absence and in the presence of 200 μM EA were recorded using a J-715 spectropolarimeter (Jasco Corporation, Tokyo, Japan) with 0.1 cm path-length quartz cuvettes. The instrument parameters were set as follows: scan rate of 50 nm min⁻¹, response of 2 s, and bandwidth of 4 nm. The background blank (neat buffer or ethanol-containing buffer) was subtracted from each sample. The recorded spectra are the results of three accumulations, and they were normalized per mole of residue. The reproducibility of the data was ensured repeating all the experiments two times with freshly prepared samples.

Isothermal titration calorimetry: ITC experiments were performed at 25 °C by means of a nano ITC III from TA Instruments (New Castle, DE, USA). The enthalpy change of binding, ΔH_b° , was determined as follows. A solution of EA, at the concentration of 100 μM, was placed in the calorimetry vessel (volume of 961 μL). The solutions of proteins were placed in the syringe (final volume of 250 μL, 100 μM). Then, 5 or 6 injections of 20 μL of the protein solutions were performed. Appropriate control measurements for the heat of dilution of the proteins were carried out as well and were subtracted from the measurements. The enthalpy changes were calculated by integration of the heat peaks and normalized by the amount of bound protein that can be calculated from the values of the binding constants determined by means of the fluorescence experiments. The standard Gibbs free energies of binding were calculated from the values of the binding constants using the relation $\Delta G_b^\circ = -RT \ln(K_b)$, and the standard binding entropies, ΔS_b° , were determined from the Gibbs-Helmholtz equation, $\Delta G_b^\circ = \Delta H_b^\circ - T \Delta S_b^\circ$. All the experiments were performed in 20 mM Tris-HCl buffer, at the pH of 7.4 in the absence and in the presence of ethanol (10 vol.%). All the experiments were repeated at least three times to ensure their reproducibility.

Author Contributions

N. J.-A. and R. O. performed the measurements and analyzed the data. R. O. and R. W. designed the study and wrote the paper.

Acknowledgements

The authors acknowledge funding from the Deutsche Forschungsgemeinschaft (DFG, German Research Foundation) under Germany's Excellence Strategy – EXC 2033 – project number 390677874-RESOLV. R. O. is grateful to the Italian MUR for being granted a research associated position (PON R&I 2014–2020, CUP: E65F21003250003). Open Access funding enabled and organized by Projekt DEAL.

Conflict of Interests

The authors declare no conflict of interest.

Data Availability Statement

The data that support the findings of this study are available from the corresponding author upon reasonable request.

Keywords: Keywords: binding · ellagic acid · ethanol effect · high pressure · polyphenols · saliva proteins

- [1] S. Quideau, D. Deffieux, C. Douat-Casassus, L. Pouységu, *Angew. Chem. Int. Ed.* **2011**, *50*, 586–621.
- [2] A. Bennick, *Crit. Rev. Oral Biol. Med.* **2002**, *13*, 184–196.
- [3] A. Rinaldi, L. Moio, in *Winemaking: Stabilization, Aging Chemistry and Biochemistry* (Eds.: F. Cosme, F. M. Nunes, L. Filipe-Ribeiro), IntechOpen, **2021**.
- [4] E. J. Dufourc, *Biochim. Biophys. Acta Biomembr.* **2021**, *1863*, 183670.
- [5] O. Cala, E. J. Dufourc, E. Fouquet, C. Manigand, M. Laguerre, I. Pianet, *Langmuir* **2012**, *28*, 17410–17418.
- [6] C. Simon, I. Pianet, E. J. Dufourc, *J. Pept. Sci.* **2003**, *9*, 125–131.
- [7] D. Roy, S. Dutta, S. S. Maity, S. Ghosh, A. S. Roy, K. S. Ghosh, S. Dasgupta, *J. Lumin.* **2012**, *132*, 1364–1375.
- [8] S. Pal, C. Saha, M. Hossain, S. K. Dey, G. S. Kumar, *PLoS One* **2012**, *7*, e43321.
- [9] S. Soares, E. Brandão, I. García-Estevéz, F. Fonseca, C. Guerreiro, F. Ferreira-da-Silva, N. Mateus, D. Deffieux, S. Quideau, V. de Freitas, *J. Agric. Food Chem.* **2019**, *67*, 9579–9590.
- [10] J. M. McRae, Z. M. Ziora, S. Kassara, M. A. Cooper, P. A. Smith, *J. Agric. Food Chem.* **2015**, *63*, 4345–4352.
- [11] B. González-Muñoz, F. Garrido-Vargas, C. Pavez, F. Osorio, J. Chen, E. Bordeu, J. A. O'Brien, N. Brossard, *J. Sci. Food Agric.* **2022**, *102*, 1771–1781.
- [12] K. A. Majorek, P. J. Porebski, A. Dayal, M. D. Zimmerman, K. Jablonska, A. J. Stewart, M. Chruszcz, W. Minor, *Mol. Immunol.* **2012**, *52*, 174–182.
- [13] F. Liu, Y. Zhang, Q. Yu, Y. Shen, Z. Zheng, J. Cheng, W. Zhang, Y. Ye, *Food Chem. Toxicol.* **2019**, *134*, 110867.
- [14] W. Humphrey, A. Dalke, K. Schulten, *J. Mol. Graphics* **1996**, *14*, 33–38.
- [15] R. Oliva, S. Banerjee, H. Cinar, C. Ehrt, R. Winter, *Sci. Rep.* **2020**, *10*, 8074.
- [16] K. A. Connors, in *Binding Constants: The Measurement of Molecular Complex Stability*, Wiley, New York, **1987**.
- [17] C. P. Woodbury, in *Introduction to Macromolecular Binding Equilibria*, CRC Press, Boca Raton, **2008**.
- [18] A. Kamali, N. Jahmide-Azizi, R. Oliva, R. Winter, *Phys. Chem. Chem. Phys.* **2022**, *24*, 17966–17978.
- [19] S. M. Kelly, T. J. Jess, N. C. Price, *Biochim. Biophys. Acta Proteins Proteomics* **2005**, *1751*, 119–139.
- [20] M. Campanile, R. Oliva, G. D'Errico, P. Del Vecchio, L. Petraccone, *Phys. Chem. Chem. Phys.* **2023**, *25*, 3639–3650.
- [21] R. Oliva, S. Mukherjee, M. Manisegaran, M. Campanile, P. Del Vecchio, L. Petraccone, R. Winter, *Int. J. Mol. Sci.* **2022**, *23*, 5690.
- [22] H. Yoshikawa, A. Hirano, T. Arakawa, K. Shiraki, *Int. J. Biol. Macromol.* **2012**, *50*, 1286–1291.

- [23] C. Simon, K. Barathieu, M. Laguerre, J.-M. Schmitter, E. Fouquet, I. Pianet, E. J. Dufourc, *Biochemistry* **2003**, *42*, 10385–10395.
- [24] G. D. Fasman, in *Circular Dichroism and the Conformational Analysis of Biomolecules*, Springer, Boston, MA, **1996**.
- [25] R. Oliva, R. Winter, *J. Phys. Chem. Lett.* **2022**, *13*, 12099–12115.
- [26] J.-M. Knop, S. Mukherjee, M. W. Jaworek, S. Kriegler, M. Manisegaran, Z. Fetahaj, L. Ostermeier, R. Oliva, S. Gault, C. S. Cockell, R. Winter, *Chem. Rev.* **2023**, *123*, 73–104.
- [27] R. Oliva, N. Jahmide-Azizi, S. Mukherjee, R. Winter, *J. Phys. Chem. B* **2021**, *125*, 539–546.
- [28] N. J. Baxter, T. H. Lilley, E. Haslam, M. P. Williamson, *Biochemistry* **1997**, *36*, 5566–5577.
- [29] J. E. Ladbury, G. Klebe, E. Freire, *Nat. Rev. Drug Discovery* **2010**, *9*, 23–27.
- [30] R. Liu, P. Qin, L. Wang, X. Zhao, Y. Liu, X. Hao, *J. Biochem. Mol. Toxicol.* **2010**, *24*, 66–71.
- [31] D. Mohanta, M. Jana, *Mol. Simul.* **2018**, *44*, 1278–1290.
- [32] N. A. Avdulov, S. V. Chochina, V. A. Daragan, F. Schroeder, K. H. Mayo, W. G. Wood, *Biochemistry* **1996**, *35*, 340–347.
- [33] V. V. Khrustalev, T. A. Khrustaleva, S. V. Lelevich, *J. Mol. Graphics Modell.* **2017**, *78*, 187–194.

Manuscript received: July 25, 2023

Accepted manuscript online: September 11, 2023

Version of record online: October 24, 2023